TABLE OF CONTENTS (TOC)

Enhanced composite thermal conductivity by presetting interconnected networks of in situ confined-grown carbon nanotubes.

Xiao Zhang*, Wei Tan, Tian Carey, Bo Wen, Delong He, Adrees Arbab, Alex Groombridge, Fiona Smail, Jean de La Verpilliere, Chengning Yao, Yanchun Wang, Xiaojun Wei, Huaping Liu, Sishen Xie, Felice Torrisi, Michael De Volder*, Weiya Zhou*, Adam Boies*

[1] Institute of Physics, Chinese Academy of Sciences, China.
[2] Department of Engineering, University of Cambridge, UK.
[3] Cambridge Graphene Centre, University of Cambridge, UK.
[4] Université Paris-Saclay, CNRS, France.
[5] Echion Technologies, UK.
[6] Molecular Sciences Research Hub, Imperial College London, UK.
[7] Dipartimento di Fisica e Astronomia, Universita' di Catania, Italy.

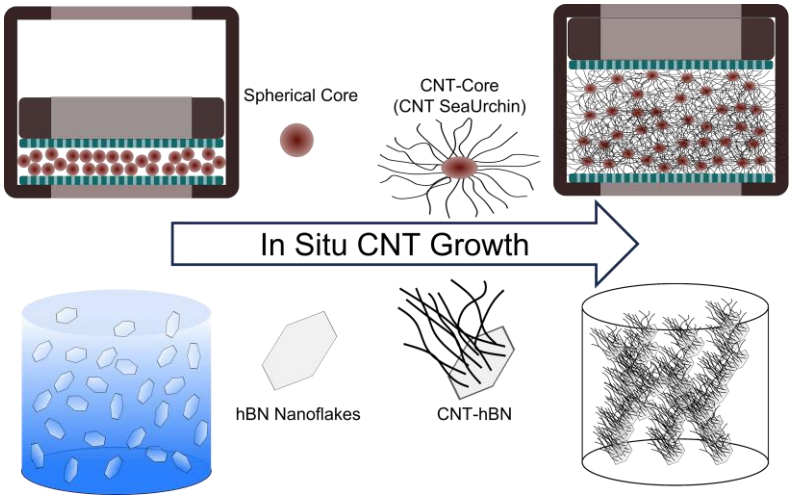

To preset an efficient 3D heat conduction network within polymer composites, we illustrated the in situ construction and persisting after compounding of the highly interconnected isotropic network with Confined-Grown CNT-cores hybrid structure and directional network with CNT-hBN nanoflakes hybrid structure.

Xiao Zhang, http://www.iop.cas.cn/rcjy/tpyjy/?id=1672

Huaping Liu, Weiya Zhou, http://nanomater.iphy.ac.cn/A05/

Michael De Volder, http://www.nanomanufacturing.eng.cam.ac.uk/Group

Adam Boies, https://amboies.com/

Nano Research

ISSN 1998-0124 CN 11-5974/O4
https://doi.org/(automatically inserted by the publisher)

Enhanced composite thermal conductivity by presetting interconnected networks of in situ confined-grown carbon nanotubes

Xiao Zhang[1,2] (✉), Wei Tan[2,†], Tian Carey[3,§], Bo Wen[2,3,‡], Delong He[4], Adrees Arbab[3], Alex Groombridge[2,5], Fiona Smail[2], Jean de La Verpilliere[2,5], Chengning Yao[6], Yanchun Wang[1], Xiaojun Wei[1], Huaping Liu[1], Sishen Xie[1], Felice Torrisi[3,6,7], Michael De Volder[2] (✉), Weiya Zhou[1](✉), Adam Boies[2] (✉)

[1] *Beijing National Laboratory for Condensed Matter Physics, Institute of Physics, Chinese Academy of Sciences, Beijing, 100190, China.*
[2] *Department of Engineering, University of Cambridge, Cambridge, CB2 1PZ, UK.*
[3] *Cambridge Graphene Centre, Engineering Department, University of Cambridge, Cambridge, CB3 0FA, UK.*
[4] *Université Paris-Saclay, Centrale-Supélec, ENS Paris-Saclay, CNRS, LMPS - Laboratoire de Mécanique Paris-Saclay, 91190, Gif-sur-Yvette, France.*
[5] *Echion Technologies, Cambridge, CB22 3FG, UK.*
[6] *Molecular Sciences Research Hub, Imperial College London, London, W12 0BZ, UK.*
[7] *Dipartimento di Fisica e Astronomia, Universita' di Catania, Catania, 64 95123, Italy.*
[†] *Present address: School of Engineering and Materials Science, Queen Mary University of London, London, E1 4NS, UK.*
[‡] *Present address: Jaguar Land Rover, Banbury Road Gaydon, Lighthorne Heath, Warwick, CV35 0RR, UK.*
[§] *Present address: School of Physics, CRANN & AMBER Research Centres, Trinity College Dublin, Dublin, D02 E8C0, Ireland.*

Received: day month year / **Revised:** day month year / **Accepted:** day month year (automatically inserted by the publisher)

ABSTRACT

Despite the ever-increasing demand of nano fillers thermal enhanced polymer composites with higher thermal conductivity and irregular geometry, nanoparticulates like carbon nanotube (CNT) have been constrained by the nonuniform dispersion, difficulty in construct effective 3D conduction network with low loading. Herein, we illustrated the in situ construction of CNT based 3D heat conduction networks with isotropic or specific preferred heat conduction performances. First, with spherical cores as support materials, we developed a confined-growth technique for CNT-core sea urchins (CNTSU) materials to in situ construct a highly interconnected isotropic conduction network. With 21.0 wt% CNTSU loading, the thermal conductivity of composites reached 1.43±0.13 W/(m•K). Secondly, with aligned hexagonal boron nitride (hBN) as anisotropic support, we constructed aligned CNT-hBN networks by in situ CNT growth, which improved the utilization efficiency of high density hBN and reduced the thermal interface resistance between matrix and fillers. With ~8.5 wt% loading, the composites possess thermal conductivity up to 0.86±0.14 W/(m•K), 374% of that for neat matrix. Due to the uniformity of CNTs in hBN network, the synergistic thermal enhancement from 1D+2D hybrid materials becomes more distinct. Based on each experimental evidence, the importance of presetting and persisting the uniformly interconnected heat conduction 3D network can be observed, particularly compared with the traditional direct-mixing method. This study can open new possibilities for the preparation of high-power-density electronics packaging and interfacial materials when both directional thermal performance and complex composite geometry are simultaneously required.

KEYWORDS

carbon nanotubes; hexagonal boron nitride; thermal conductivity; composites; 3D printing

1. Introduction

With the rapid progress of autopilot, battery management, and 5G technology, heat dissipation from high-power-density electronics and associated packaging or interfacial materials have become increasingly critical on guaranteeing electronics performance and reliability [1-4]. The heat dissipation components need to be easily manufactured, highly thermally conductive, lightweight, and geometry adaptive [2]. For these purposes, commonly used polymer materials have ever been enhanced by mixing with micro or nano fillers with high thermal conductivity (κ), such as carbon nanoparticles [5-11], boron nitride [12-16], and other ceramic particles [4], particularly by direct-mixing, to improve the thermal conductivity of resulting

Address correspondence to X. Zhang, zhangx@iphy.ac.cn; M. De Volder, mfld2@cam.ac.uk; W. Zhou, wyzhou@iphy.ac.cn; A. Boies, amb233@cam.ac.uk

composites (κ_{CP}). Among these fillers, carbon nanotubes (CNT) has attracted special attention due to the intrinsic high thermal conductivity (κ ~ 3000 W/(m•K)) and high aspect ratio thus facilitating forming efficient heat conduction pathway within polymer matrix [17]. However, commonly only modest κ_{CP} increase had been obtained, mostly because of filler being isolated and randomly distributed at low loading during the process of being mixed with polymer and curing, thus impeded by poorly conductive polymer (κ=0.1-0.2 W/(m•K)) in building an closely interconnected network, as well as the contact resistance between the fillers and the high interfacial thermal resistance between fillers and surrounding polymer matrix [18]. Nevertheless, higher CNT loading significantly increases the processing challenge due to the dramatically increased viscosity and fillers agglomeration. Therefore, to effectively increase κ_{CP}, a preset 3D interconnected CNT network in composite is essential, which can survive the compounding process and occupy increased fraction in a matrix [17].

In our previous research, with in situ polymerization, CNT sheets fabricated by stacking thousands of CNT films produced by continuous CVD were used as the filler [19]. The preset heat conduction network from CNT sheet endows composites with high κ_{CP}, even though only along the in-plane direction due to the highly anisotropic conductivity of multi-layered CNT sheet (in-plane κ ~120 W/(m•K) and the normal direction κ ~0.1 W/(m•K)). Moreover, extensively explored as thermal interface materials, CNT vertical array (CNT forests) can achieve high κ_{CP} in normal direction of sheet composites, but their geometries are still limited by the array dimension scale. Thus, to construct the 3D interconnected CNT networks with flexibility on geometry and either isotropic or preferred directional thermal performance motivated us to in situ grow CNT on proper support for presetting the efficient heat conduction pathway.

Herein, we adopted spherical cores and hexagonal boron nitride (hBN) 2D materials as support materials to in situ preset CNT based isotropic and anisotropic 3D interconnected networks, respectively. With spherical cores as support, the hybrid CNT-cores sea urchin (CNTSU) structure has been synthesized within a confined space to form a highly interconnected bulk material, with which high and uniform filler loading can be realized in synthesis of enhanced isotopically thermal conductive composites. On the other hand, with hBN as support, an in situ grown aligned CNT-hBN network was prepared with uniform hybrid distribution and used in constructing the anisotropic thermal conduction composites. To deal with the problems of relative high density and low aspect ratio for hBN powder, by using a directional ice-templating self-assembly method, the utilization efficiency of hBN and uniformity of hybrid fillers has been improved with lower filler loading (<10 wt%). In the end, the 1D+2D synergistic effects [5, 20, 21] from CNT-hBN hybrid nanoparticulates have also been discussed.

2. Experimental details

2.1 Confined-Growth of Hybrid CNT-cores (CNT Sea Urchin) Highly Interconnected Isotropic Networks.

The cores to grow CNTSU were continuously synthesized by our previous reported spray-drying method [22]. Briefly, aqueous solution of aluminium nitrate and iron nitrate was atomized with nitrogen carrier gas to form micron droplets aerosol which then in-line dried and calcinated to become aerosol of micron hollow cores with iron islands randomly distributed among alumina.

Following our previous report, the CNTSU can be continuously grown in-line (referred as Continuous-Growth) [22] and freely grown ex situ on the substrate (referred as Free-Growth). However, for seeking high CNT density and closely interconnected CNTSU fillers, we developed the Confined-Growth method to confine the expending CNTSUs during growth and fill the mold (Figure 1a).

The key of Confined-Growth is the porous and demountable growth cage (Figure 1b,d and Figure S1 in the ESM) which is 3D printed with the Form2 SLA 3D Printer equipped with the ceramic resin (SiO_2 particle included). After being trimmed and fired, all the growth cage components transformed into silica ceramic texture which can tolerate the high CNT growth temperature and reaction gases.

Mixed with IPA to form slurry, cores were coated onto anodic aluminum oxide (AAO, Whatman Anodisc 47, 60 μm thick with 200 nm nominal pore size through-holes) substrate. After covered by another piece of AAO, this AAO-cores-AAO sandwich was assembled with the growth cage, and inserted into the CVD growth furnace set to 800℃ (Figure 1c-d). With helium as the carrier gas, the cores were firstly reduced by hydrogen for 10 min. After the flow of ethylene as the carbon source being mixed, the CNT growth started and lasted for ~1 h, and then reaction gases were flushed by pure helium before furnace being cooled down. The resulting CNTSU bulk material was strong enough to be frees-standing, and released from cage and AAO substrates (Figure 1e-f). The thickness of final CNTSU bulk materials can be tuned by changing the thickness of ceramic covering weight & occupier and the slurry thickness.

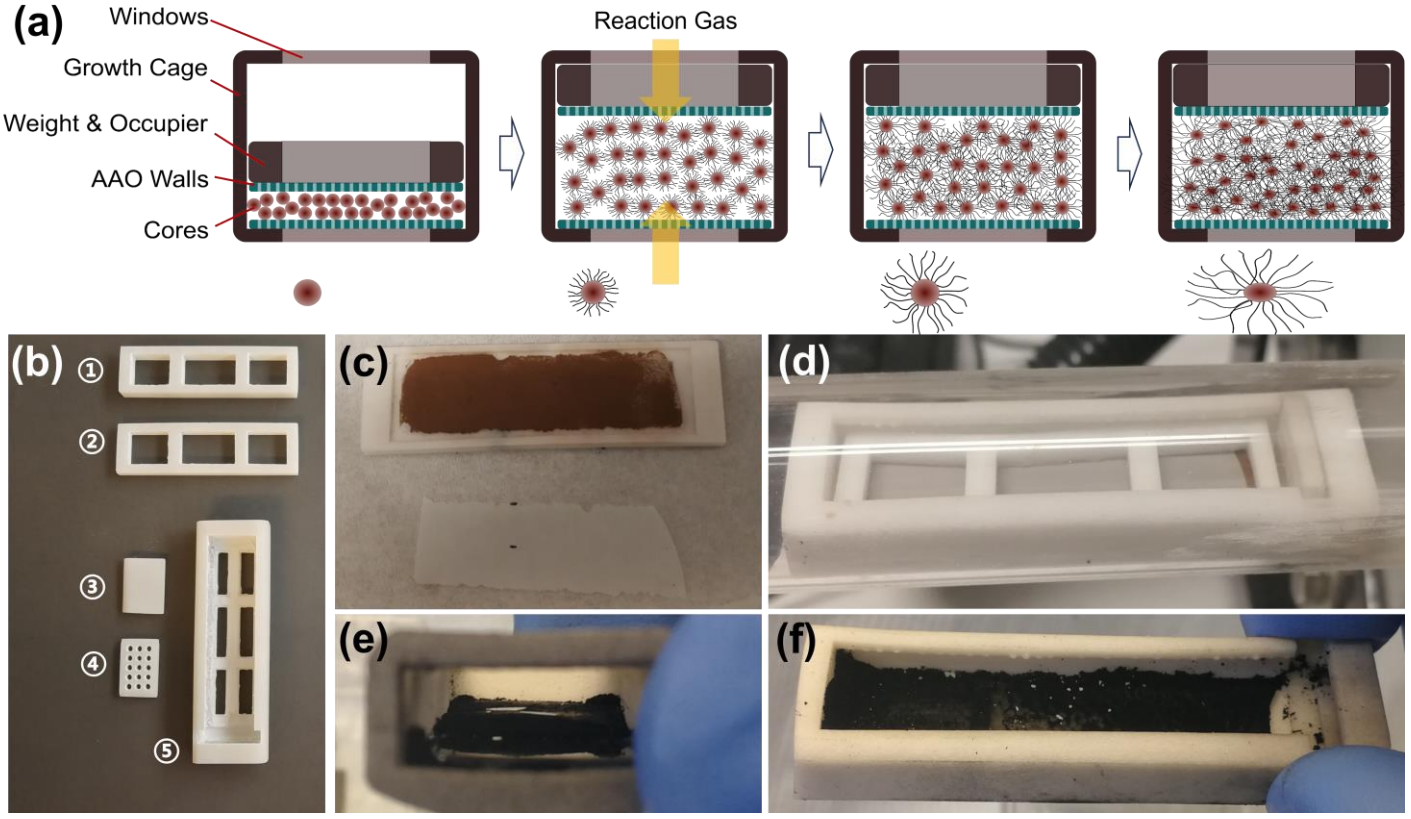

Figure 1 Confined-Growth of CNTSU with a 3D printed growth cage. (a) Schematic diagram of the Confined-Growth of CNTSU (CG-CNTSU) and the morphology evolution of individual CNTSU. (b) After being trimmed and fired, the polymer matrix within component precursors burned away, leaving the model transformed into a silica ceramic texture which can tolerate 1100℃. Within these components, ①② are the cover weight & occupier with different thickness to tune the thickness of grown bulk materials; ③④ are the mountable side walls facilitating cores loading and CNTSU unloading; ⑤ is the main body of the cage. (c-d) After the cores being blade-coated onto the bottom AAO, they were successively covered by the covering AAO, assembled with other cage components, and inserted into quartz tube for CVD growth. (e-f) After standard CNT growth process, the CG-CNTSU bulk materials were synthesized with desired thickness.

2.2 Preparation of Aligned hBN Support and In Situ Construction of Hybrid CNT-hBN Networks.

The hBN nanoflakes (hBNNFs) were produced by exfoliating hBN powders (Goodfellows B516011) within a shear fluid processor (microfluidizer, M-110P, Microfluidics International Corporation, Westwood, MA, USA) [23]. Carboxymethylcellulose sodium salt (CMC, average molecular weight = 700,000, Aldrich No. 419338) was added to stabilize the hBN in solution. The hBN solution came as an aqueous ink with hBNNFs concentration of 0.44 mg/ml. The hBNNFs' lateral size was ~520 nm, and thickness followed a log-normal distribution peaking at 9 nm.

As shown in Figure 2, a steel mold containing the inks with desired filler concentration was placed onto a large heat sink which had been cooled in advance to liquid nitrogen temperature. With a fast anisotropic freeze casting process, hBNNFs were expelled out from layered ice crystal [24], forming a well aligned network vertically along the temperature gradient. After freeze-drying (Telstar® LyoQuest Freeze Dryer) for 48 h, the aligned support network (aerogel) of pure hBN can be obtained.

While, to in situ construct the hybrid CNT-hBN network, before freeze casting, the hBNNFs ink was firstly mixed with Fe_2O_3 nanopowder (~5 nm, Alfa Aesar 044296.09) and then followed the same process to prepare the red Fe_2O_3 NP-hBN network which was used for a standard CNT growth (similar to CNTSU). The in situ grown CNT outstretched from the hBNNFs, forming the final hybrid CNT-hBN network.

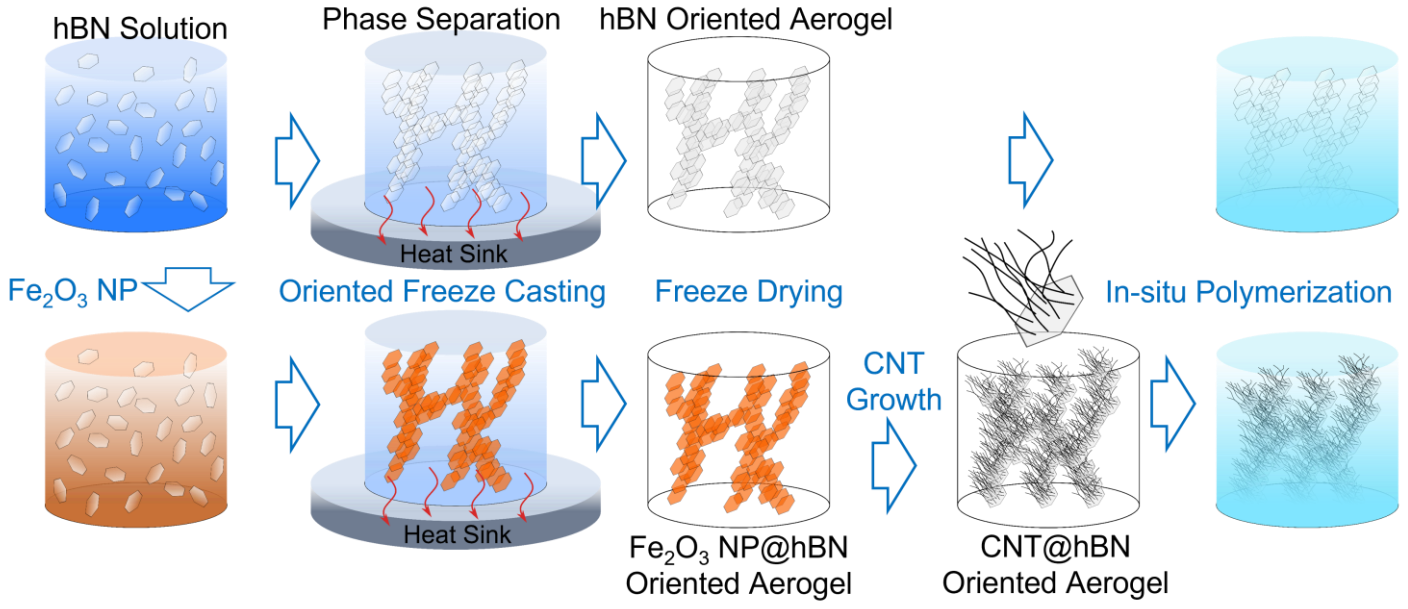

Figure 2 Preparation schematic diagram of hBN aligned network (upper row) and the in situ grown aligned CNT-hBN network (lower row) used as thermal enhancement hybrid fillers.

2.3 Preparation of Thermal Enhanced Composites by In Situ Polymerization

Both above hybrid networks were impregnated through the in situ polymerization of epoxy which had been firstly diluted with acetone and followed by evaporation of the acetone under vacuum, and by curing with a vacuum bag method as sketched in Figure 3. The epoxy resin was bisphenol-A IN2 infusion resin and a hexane hardener (Easy Composites Ltd). The epoxy resin and hardener were mixed in the proportion 10:3 by mass. By repeating the infiltration process before curing, the voids inside network can be effectively filled, benefiting from the capillary force and vacuum environment. The impregnated hybrid networks were located within a PTFE mold to tune the nominal thickness of 1-2 mm. An outer breather layer cloth, and a vacuum bagging system (Easy Composites Ltd) were used to apply a consolidation pressure of P = 0.1 MPa (one atmosphere), at a temperature of 40 °C for 1 h. Excess resin was absorbed by the breather layer cloth during consolidation. Samples were then cured at 120 °C for 3 h, with a constant pressure of 0.1 MPa to guarantee full polymerization.

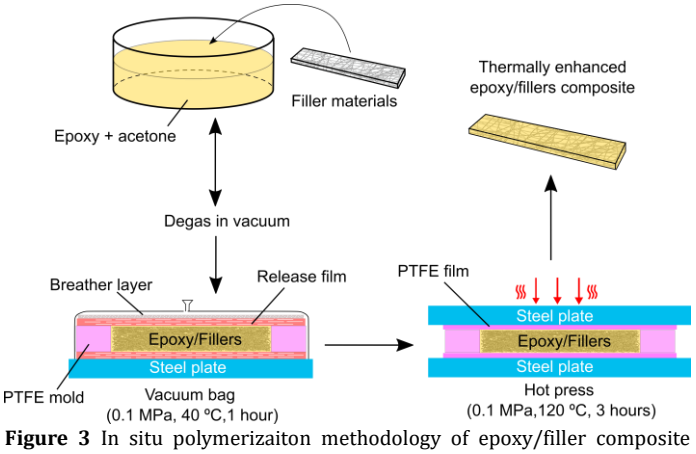

Figure 3 In situ polymerizaiton methodology of epoxy/filler composite manufactured with vacuum bag and hot press methods.

As control groups, CNTSU powders, hBN powders and hBN & CNT (NC7000, Nanocyl) hybrid powders were also used as enhancement fillers by direct-mixing. An epoxy resin with uniformly dispersed fillers was obtained by using a planetary mixer (MSK-PCV-300-LD) at 1500 r/min at room temperature for 10 min. The mixture was then degassed in the vacuum oven (ACROSS INTERNATIONAL Elite series) for 1 h and then cured. Polypropylene (PP, Borealis, Belgium)/CNTSU composites were also manufactured using a twin-screw micro extruder (DSM Explore 5 cc Micro Compounder, DSM) for mixing 20 min at 210 °C with the speed of 60 rpm. The composite samples were fabricated via the extrusion-injection method (Micro 5 cc Injection Molder, DSM, Xplore Instruments). The temperatures of the injection nozzle and mould holder were set at 210 °C and 55 °C, respectively. κ of PP was measured to be 0.22±0.1 W/(m•K), nearly the same with the measured value of epoxy matrix used.

2.4 Characterizations

κ_{CP} were measured according to the ASTM D5470-17 standard using a custom-made steady-state measurement setup (Figure S2a) based on the Bi-substrate technique [19]. Square specimen with sides of 10 mm were placed between hot and cold copper blocks which were used as heat flux meters. According to Eq.1, κ of specimen through thickness at ~37°C and R_i between specimen and heat flux meters can be directly deduced by linear fitting data obtained from samples with different thickness (Δz):

$$\Delta T/q=\Delta z/\kappa+2/R_i \quad (1)$$

where ΔT was the total temperature drop, q was heat flux through sample. Considering the practical engineering application demand, referential errors were calculated by the stochastic error propagation method, generating confidence limits for each calculated κ value. Briefly, during every round of calculation iteration, κ was deduced with a new set of random parameters which were generated based on geometric and thermal parameters' expected values, experimental random/

systematic errors, and distribution style.

The SEM images were conducted on a field-emission SEM (TESCAN MIRA3). The fracture surfaces of composites were prepared by being cryo-fractured in liquid nitrogen and sputter-coated with a thin layer of gold in a vacuum chamber before SEM observation. Thermogravimetric analysis was conducted with the PerkinElmer Pyris 1 TGA in flowing air environment at 10 K/min heating rate.

3. Results and discussion

3.1 Composites Thermally Enhanced by Hybrid CNT-Cores Structure (CNTSU).

3.1.1 CNTSU Morphology and Its Thermal Enhancing Performance by Direct-mixing

By using a continuous aerosol process, the alloy micron cores of alumina and iron oxides can be industrial-scale produced (Figure 4a). The size range of these hollow cores is 0.2–5 μm (mostly 1-2 μm). Because these cores are hollow with shell thickness of several nanometers [22], they can be easily crushed into debris under pressure. With 20 mins of free-growth without any space confinement, CNTs were radially grown from embedded iron crystallites on cores to form the hybrid CNT-cores sea urchin (CNTSU) structure. The diameter of CNTSUs grown for 20 mins is 4-10 μm (Figure 4b) compared with 1-2 μm cores used. With free-growth method, CNTSUs powders were prepared with loose interconnection by the outstretching and entangled CNTs.

Compared with other reported CNTSU structure [25], the CNT percentage for our CNTSU is much higher due to dense distributed catalysts sites instead of only decorating tiny amount of catalysts on the cores surface. For the instant in-line CNTSU growth (Continuous-Growth), the CNT weight percentage is ~40 wt% [22]. By increasing the growth time, larger CNTSU with more surrounding CNTs were grown (Figure S3). With 0.3 h, 1 h and 4 h of free-growth, the CNT weight percentage increases to ~73.8 wt%, ~91.2 wt% and ~94.3wt%, respectively, based on the TGA results. However, as the growth time increased to 4 h, grown CNTs tent to curl up into wisps instead of continuing expanding and outstretching.

As control groups, we firstly direct-mixed CNTSU within matrix to thermally enhance composites, because CNTSU powders with looser CNTs and higher cores percentage has been reported to owe remarkably low thermal percolation threshold (~0.15 wt%) by direct-mixing method [25]. By using a twin-screw extruder and injection molding, PP/CNTSU composites had been synthesized with higher loading. As shown in Figure 5, the ever increase of thermal enhancement by increasing filler loading can be easily identified. When 10 wt% of CNTSU was added, thermal conductivity of enhanced composite κ_{CP} reached 0.44±0.01 W/(m•K). Moreover, the higher κ_{CP} from longer CNT growth time thus higher CNT percentage can also be observed when the same 2 wt% of CNTSU were added. However, the mild κ_{CP} increase from 4 h grown CNTSU compared with that grown for 1h prompts us to choose 1 h for the following experiments as the sufficient growth time for CNTSU to expand. Composites with CNTSU filler loading higher than 10 wt% were hindered by the low viscosity to form a uniform dispersion of CNTSU with the direct-mixing.

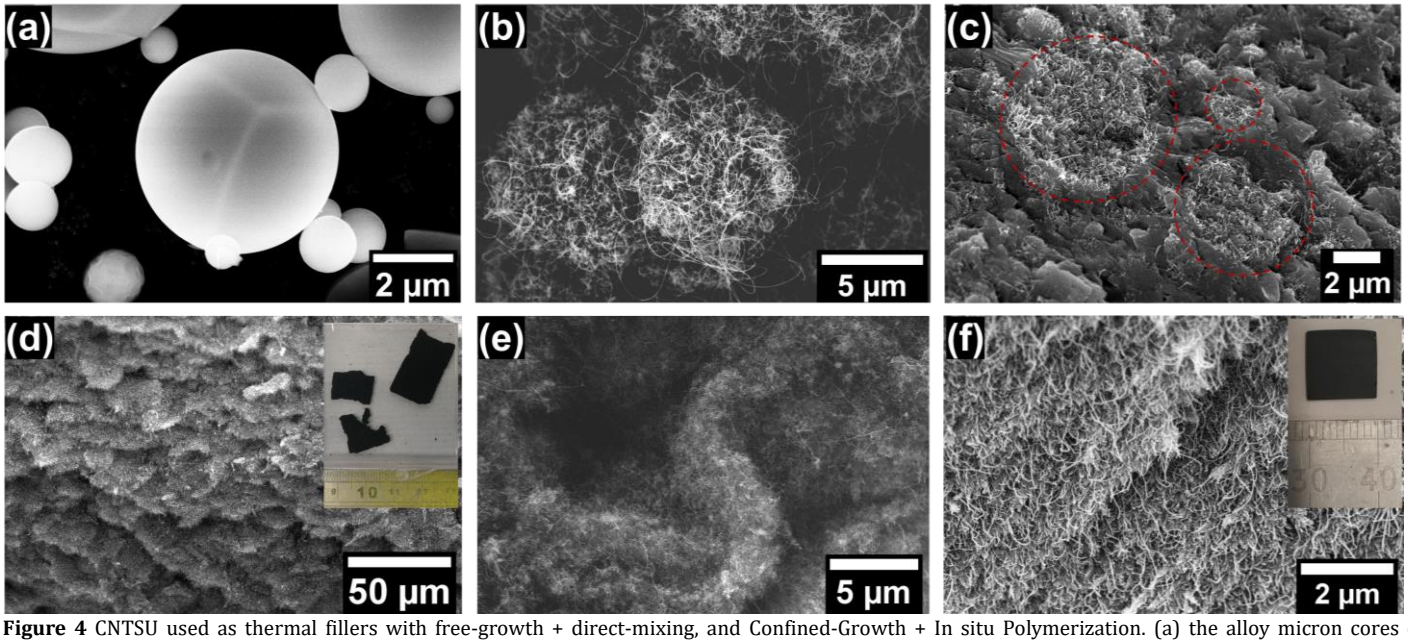

Figure 4 CNTSU used as thermal fillers with free-growth + direct-mixing, and Confined-Growth + In situ Polymerization. (a) the alloy micron cores of aluminium and iron oxides synthesized with a continuous aerosol process. (b) With 1 h of free growth under unlimited expansion, the CNTSU morphology formed with CNT outstretching, expanding the diameter compared with cores. (c) By direct-mixing with a twin-screw extruder, in the final composites, the dispersed CNTSU shrunk on diameter, and even 10 wt% of loading cannot guarantee the close interconnection between CNTSUs. (d-e) With custom-made growth cage, the expansion space had been confined for the growing CNTSU, forming the Confined-Grown CNTSU (CG-CNTSU) bulk material (photo inset). During this process, the hollow cores were crushed into oblate spheroids. CNTs among different CG-CNTSUs entangled, forming the hierarchical interconnected 3D network. (f) With CG-CNTSU and in situ polymerization, 21 wt% high filler loading can be easily realized with preset CNT interconnection persisted within the final composite (photo inset).

Nano Research
ISSN 1998-0124 CN 11-5974/O4
https://doi.org/(automatically inserted by the publisher)

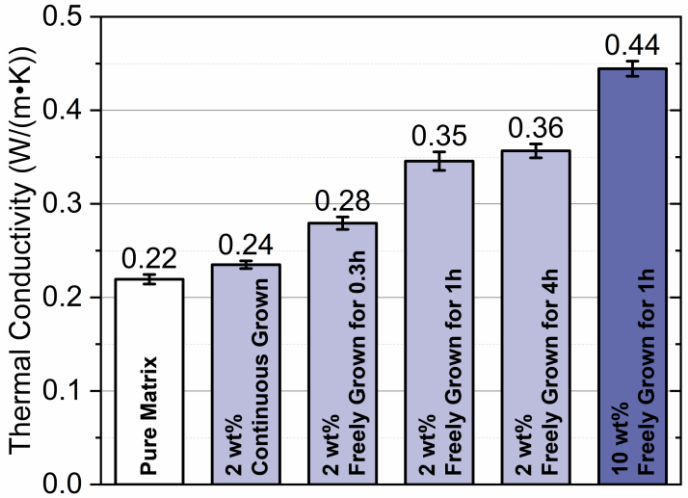

Figure 5 The mild thermal enhancement from CNTSU by direct-mixing with different filler loading and CNTSU growth time.

However, as shown on the fracture surface of above composites (Figure 4c and Figure S3), by direct-mixing, CNTSUs have not constructed interconnected network, instead CNTSU isolated distributed even for 10 wt% loading. Moreover, direct-mixing also tended to shrink the outstretching of CNT formed during growth, when compared the diameter change before and after compounding. An efficient heat conduction network cannot be easily reached. Consequently, low thermal conductive matrix between CNTSU and the high Kapitza resistance at the CNT/matrix interface [26] hindered the heat transfer. To further increase κ_{CP}, presetting a closely interconnected network of CNTSU, as well as increasing the density and uniformity among bulk material become essential.

3.1.2 Closely Interconnected Network Based on the Confined-Grown CNTSU.

As shown in Figure 1, the ceramic growth cage prepared by 3D printing combined with the porous AAO walls confined the disorderly expansion of CNTSU during the growth process, forming uniformly compacted CNTSU bulk materials with desired thickness. Based on our previous experiment, reaction gases cannot penetrate through compacted CNTSU thicker than 5 mm. Therefore, we applied the AAO as the confining wall, which can tolerate growth environment and thin enough for the feeding of reaction gas to supply the growth of CNT through the nanopores on the AAO. As growth start, the expansion of CNT lifted the weight to the maximum allowed space. Then the ever expansion forced CNTs to entangle inward. As the CG-CNTSU squeeze with each other, the original sphere cores cannot be observed within final material anymore, instead the thin shells of hollow cores were easily crushed into oblate spheroid and debris, finally building the closely interconnected high-density CNTSU bulk material (Figure 4d-e), referred as the Confined-Grown CNTSU (CG-CNTSU). CNTs among different CNTSUs entangled, forming the isotropic and interconnected network. The density of the CG-CNTSU with 1 h growth is ~0.20 g/cm^3. Owe to the close interconnections between CNTSUs, the CG-CNTSU bulk material is free-standing (photo inset Figure 7d), which facilitates handling as a preset thermal conduction network.

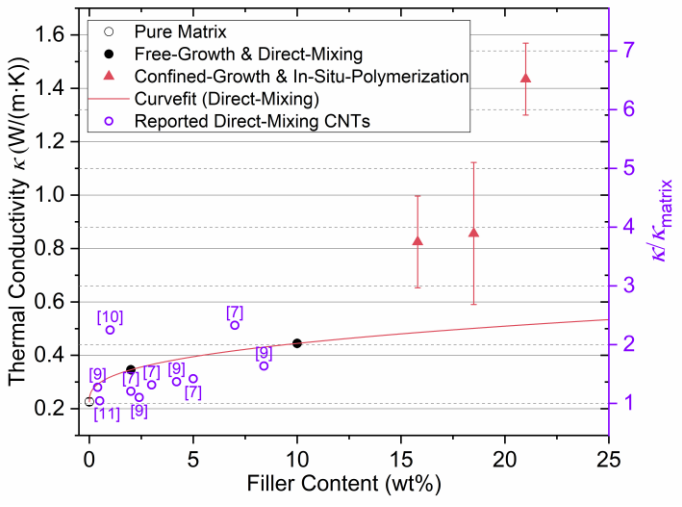

Figure 6 The optimized thermal enhancement from the Confined-Grown CNTSU and the in situ Polymerization. The κ_{CP} enhancement from the closely interconnected CG-CNTSU is much significant which overtake the prediction of the power-law curve fitting of results from the direct-mixing. The reported CNT thermally enhanced composites were also listed (purple hollow circles) according to their enhancement factor compared to corresponding matrix (compared with right-axis). Colorful version online.

By using CG-CNTSU as filler and further combined with in situ polymerization, the epoxy/CG-CNTSU composite has been synthesized. With the preset highly interconnected heat conduction networks, the CNTSU loading easily surpassed 15 wt%. More importantly, as shown in Figure 6, when the filler loading is 15.8 wt%, κ_{CP} of epoxy/CG-CNTSU composite reached 0.82±0.17 W/(m•K). κ_{CP} further increased to 1.43±0.13 W/(m•K) for 21.0 wt% of loading, 6.2 times higher than that of the neat epoxy matrix (0.23± 0.01 W /(m•K)). The thermal enhancement from the CG-CNTSU and in situ polymerization all surpass the prediction from the power-law curve fitting based on results from the direct-mixing. From the fracture surface of epoxy/CG-CNTSU composites (Figure 4e), in situ polymerization process indeed persisted the dense CNT interconnection formed during growth. Consequently, more pathways are available for phonons when traverse through the composite, giving rise to the thermal enhancement. Above evidence emphasizes the importance of the presetting and persisting closely interconnected heat conduction network.

3.2 Composites Thermal Enhanced by the In situ Grown Aligned Hybrid CNT-hBN Networks.

3.2.1 Thermal Enhancement by Aligned hBN Network with Low Loading.

As we discussed in the introduction section, to construct a 3D closely interconnected heat conduction network with CNT materials, we used the cores as support in building an isotropic network (CNTSU bulk materials) and breaking the loading upper limit. While to in situ construct an anisotropic network with preferred heat conduction direction, we used the anisotropic nanoparticulates like 2D materials as support to in situ grow CNT.

Although graphene as the best thermal conductive 2D materials (in-plane $\kappa_{\parallel}$~3000 W/(m•K)), we have not achieved any competitive results with graphene as support materials (brown solid pentagon in Figure 7). We have tried to use graphene oxide (GO) solution based method and in situ reduction and CNT growth in building heat conduction network (Figure S4). We attribute the poor thermal enhancement to the highly defective graphene obtained after reduction GO aerogel and CNT growth. The phonon scattering from defects and crystal boundary might be too serious, hiding the thermal enhancement. Additionally, with current growth parameters, growing CNT from iron catalyst attached on graphene substrate seems to be inefficient. Only short and curly CNT can be observed. Iron catalysts seem to deteriorate the rGO surface by etching at high temperature and reduction environment [27, 28].

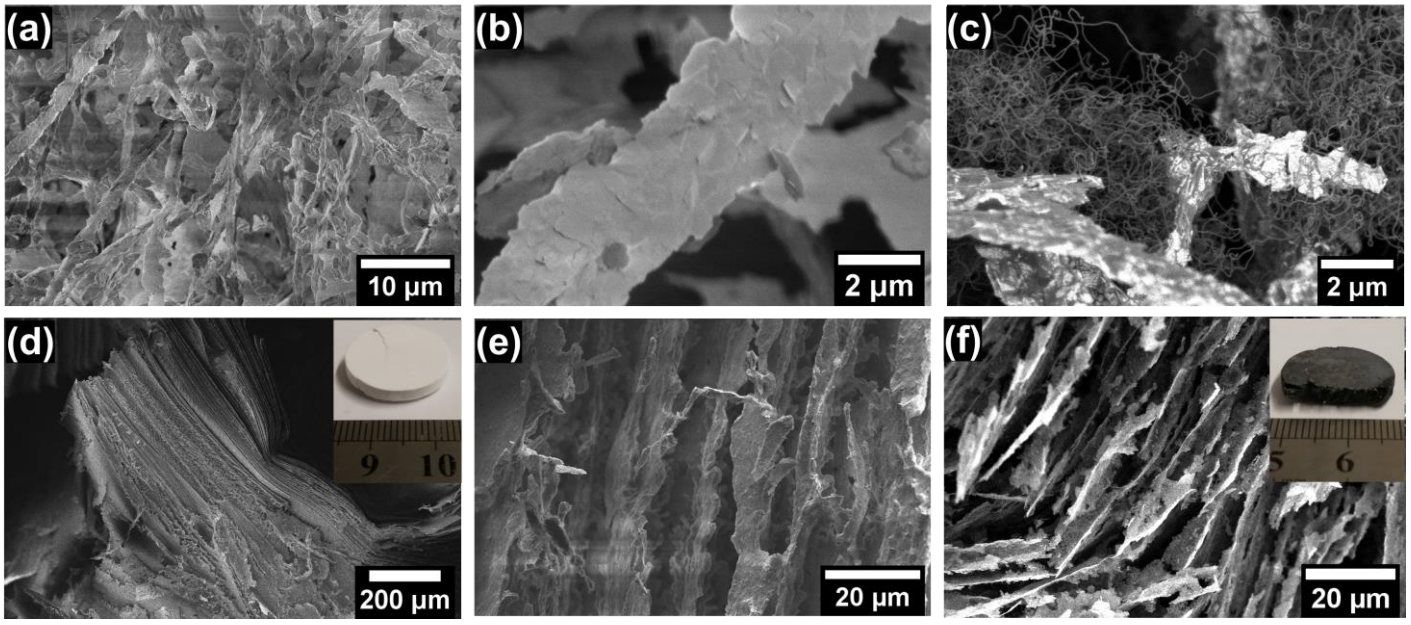

Figure 7 In situ Grown aligned CNT-hBN network used as thermal enhancement hybrid fillers. (a-b) With low concentrated hBN solution (0.44 mg/ml) and directional ice-templating self-assembly method, the hBNNFs self-assembled into aligned hBN nanobelts within the network. (d-e) By further concentrating the hBN solution to ~3.5 mg/ml, the resultant nanobelts become thicker, wider, and denser, finally forming the aligned porous nano-book network (photo inset). With the aligned hBN network as support materials, CNTs were in situ CVD grown from iron catalysts and extended outward from hBN support, interconnecting inter and intra hBNNBs through the thickness as illustrated in the fracture surface of both (c) low and (f) high density network. After the CNT growth, the hybrid network still retained free-standing state as shown in inset photo.

Therefore, we tend to hBN as the anisotropic 2D support materials, because of its high temperature resistance, chemical inertness, and outstanding in-plane thermal conductivity ($\kappa_{\parallel}$~360 W/(m•K)) [29]. However, due to the relative high density of hBN, the micron scale size and the anisotropic κ for individual hBNNF, proper orientation and connection among hBNNFs becomes essential to fully utilize their higher in-plane $\kappa_{\parallel}$ instead of out-of-plane $\kappa_{\perp}$~ 30 W/(m•K), as well as to construct more efficient thermal conduction network with much lower filler loading (<10 wt%) rather than commonly used 30-60 wt% [13, 30, 31] which brought in excessive density/weight increase.

As shown in Figure 2, we utilized directional ice-templating self-assembly and freeze-drying method to organize highly delaminated thin layer hBN. Due to the aligned ice crystal growth arising from the imposed vertical temperature gradient, an aligned hBN network was prepared (Figure 7a). Take the advantage of the highly delaminated hBN produced with shear fluid processor, hBN nanoflakes overlapped with each other along the crystal in-plane direction, and finally self-assembled into the hBN nanobelt (hBNNB, Figure 7b). In contrast to other normal freeze-drying method, this directional self-assembly method changes the aerogel as a thermal insulation material composed with randomly distributed hBN. By further concentrating the hBN solution to ~3.5 mg/ml, hBNNBs become thicker, wider, and denser in aligned network, finally forming the porous aligned nano-book (Figure 7d-e).

Owing to the aligned hierarchical organization of hBN, a more efficient thermal conduction network had been built with a low filler loading (2-7 wt%). With in situ polymerization, the prepared epoxy/aligned hBNNB composites retained the geometry and uniformity of the hybrid network. As can be observed in Figure 8 (blue hollow diamond), with 2.5 wt% and 6.6 wt% addition of aligned hBN aerogel, κ_{CP} along the desired direction (through thickness) reached 0.29±0.01 W/(m•K), 0.43±0.02 W/(m•K), respectively. As a comparison, by direct-mixing hBN powder within matrix, κ_{CP} is only 0.29±0.01 W/(m•K), 0.38±0.03 W/(m•K) when the loading is 6.5 wt% and 12.0 wt%. In Figure 8, the difference of curve fitting trend between the 2 sets of results emphasizes the importance of the delamination process and the well alignment of hBN within hBNNBs. When compared with reported results also based on aligned hBN fillers (purple diamond) but produced with ball-milling [12] or CVD method [16], our results are still superior at similar loading. We attribute this superiority to the higher aspect ratio (AR>55) of the used hBNNF produced by shear fluid processor [23] than the sonication ones (AR~20,

typically 200 nm lateral size, 10 nm thick). This is because with larger lateral size and AR>40, the nanoflakes tend to align [32] and construct ordered overlapping within nanobelts, the superior in-plane thermal conduction of hBN can thus be better utilized in the conduction pathway. With much reduced interface density along conduction direction, phonons scattering in all directions as happened to random system can be avoid. Meanwhile, with an improved alignment, the contact area between hBNs would further extended, thus decreasing the contact resistance between hBNs [18]. Therefore, along the axis of hBNNBs, nanoflakes possessing high $\kappa_{\parallel}$ could form an "express highway" to channel the heat. With the enhanced thermal conductivity, the aligned pure hBN composites are indispensable for the application with purposes of both electric insulation and thermal conduction.

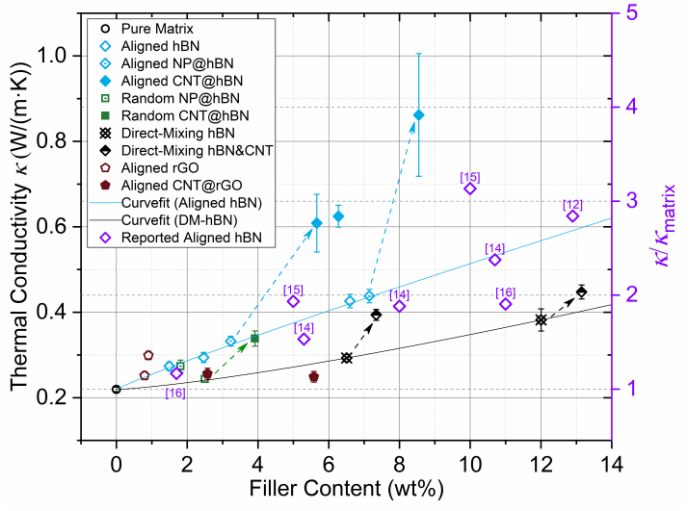

Figure 8 The thermal enhancement from the hBN associated filler and the aligned hybrid CNT-hBN network. Networks of aligned pure hBN and the in situ grown hybrid CNT-hBN acted as superior thermal enhancement fillers than the random distributed hBN networks and control groups with direct-mixing. The synergistic effect from the 1D+2D nanomaterials can also be identified on the CNT-hBN systems particularly for the in situ grown ones. The reported composites results enhanced by aligned hBN were also listed as purple hollow diamond, which should be compared with the right axis. All the other data points were experimental results in this work. Some trials on CNT-graphene network were also presented (More details can be found in Figure S4 in the ESM). Colorful version online.

3.2.2 Synergistic Effect on the In situ Grown Hybrid CNT-hBN Aligned Network.

With the above aligned hBN network as support material, we constructed the anisotropic network of hybrid CNT-hBN by in situ CNT growth. As shown in Figure 2, by simply mixing iron oxide as catalysts within hBN solution, the Fe_2O_3 NP can be easily distributed within hBN network after freeze drying. With further in situ CVD growth, CNTs synthesized from iron catalysts outstretched, and interconnected inter and intra hBNNBs within networks of both low and high density (Figure 7c and f). After the CNT growth, the CNT-hBN aerogels still retained sufficient mechanical strength and free-standing state (photo inset Figure 7f). It is worth noting that we have also tried to build CNTSU-hBN hybrid network, however, because of the occupying effect from micron cores, the core-hBN aerogel was too brittle to be free-standing.

By using this hybrid CNT-hBN networks as fillers, the resultant epoxy/CNT-hBN composites show a higher κ_{CP} than those with similar hBN loading. As shown in Figure 8 (blue solid diamond), with ~5.7 wt% loading (~2.9 wt% hBN and ~2.7 wt% CNT), κ_{CP} reached 0.61±0.07 W/(m•K), higher than 0.33±0.01 W/(m•K) for the similar hBN loading (~3.0 wt% hBN and ~0.3 wt% Fe_2O_3 NP). The highest κ_{CP}=0.86±0.14 W/(m•K) came from the ~8.5 wt% hybrid filler among which ~6.6 wt% hBN and ~1.4 wt% CNT), 374% of that for neat matrix. When compared with reports results, similar κ_{CP} (0.85 W/(m•K)) can only reached with vertically aligned hBN–epoxy composites with 20 wt% hBN loading [15].

In recent years, the synergistic effects of simultaneously using 2D (graphene, hBN, etc.) and 1D (CNT, nanofiber, etc.) nanoparticulates have been discovered [5, 20, 21]. As shown in Figure 8 (blue symbols), the κ_{CP} for the hybrid network were higher than the prediction from the curve fitting based on the aligned pure hBN ones. The corresponding thermal enhancement cannot either be achieved with only the similar loading of CNTs (2.7 wt% or 1.4 wt%). As shown in Figure 6 (purple circles), according to the reported results [7-11, 33], the thermal enhancement factor from <3 wt% loading of CNT were always <50%, or <0.057 W/(m•K) the absolute value for epoxy matrix. All these evidence indicates the formation of a synergistic thermal enhancement effect between 1D CNT and 2D hBN. The thermally bridging hBN 2D nanoflakes with 1D CNTs, extending the conductive 1D-2D hybrid network, increasing the total interfacial area by increasing the filler dimensions, combined with the high cross-plane transmission of phonon modes between CNT and hBN [34], leading to reduction of the thermal interface resistance (R_i) along the network [5]. Additionally, without CNT growth, epoxy/Fe_2O_3 NP-hBN composites did not show similar synergistic thermal enhancement effect (blue dotted diamond), instead κ_{CP} seems to follow the prediction based on the pure hBN, emphasizing the contribution from CNTs to interconnect neighbouring hBN, where the synergistic effect originated.

The synergistic thermal enhancement from CNT-hBN random network can also be observed (green solid square), however, limited by the inefficient conduction through randomly distributed hBN, the thermal enhancement was not remarkable. Moreover, similar synergistic enhancement trend can also be observed from direct-mixing by stirring hBN powders with NC7000 CNT powders within epoxy resin: both hybrid fillers (half black diamond) show the superior enhancement from the curve fitted prediction based on the direct-mixed only hBN within a matrix, but the increase in slope is milder compared with that from in situ grown CNT and with similar CNT loading. This should originate from the nonuniform dispersion of the hybrid fillers and the curling up of CNTs by direct-mixing [35]. The high contact resistance between fillers was also generated by tiny contact area and weak interaction between hBN and CNT by direct-mixing [30]. Therefore, both in situ constructing highly interconnected and uniform 1D+2D hybrid network and aligned organization of fillers seem to be essential in realizing an efficient synergistic thermal enhancement effect.

On the other hand, because for both CNT-cores and CNT-hBN hybrid networks mentioned in this work were

constructed by casting in a mold, we can expect to achieve thermal enhanced composites with irregular shapes by in situ polymerizing the in situ grown irregular shaped network with preset thermal conduction performance. For hybrid CNT-cores network, since the CG-CNTSU bulk material is derived from the growth and expansion of CNT, the shape of the bulk material can cast the shape of cage space. While for hybrid CNT-hBN network, the freeze-casting and freeze-drying process guaranteed the network to cast the shape of mold. Combined with in situ polymerization to persist the network after compounding, the advantage of irregular manufacturing of injection molding by direct-mixing can still be retained while the troublesome dispersing of filler within matrix can be avoided.

4. Conclusions

To thermal enhance polymer composites with nanoparticulates like CNTs, we found the importance of presetting the closely interconnected CNT heat conduction network and persisting this network after compounding process. By using micron cores and hBN nanoflakes with high aspect ratio as support materials, we successfully constructed the 3D interconnected hybrid CNT-support network by in situ CNT growth, forming the desired isotropic or preferred heat conduction performances. More specifically, with cores as the support, we developed an in situ confined-growth technique for CNT-core (CNTSU) materials to construct an isotropic network as efficient phonon transport pathway, which easily surpassed 15 wt% loading limitation and solved the nonuniform filler dispersion and agglomeration problem for traditional direct-mixing method. When the loading further increased to 21.0 wt%, the thermal conductivity of composites reached 1.43±0.13 W/(m•K). On the other hand, with high AR hBN as the support, we constructed an aligned hybrid CNT-hBN network by in situ CNT growth. With relative low loading (~8.5 wt%) of hybrid filler to avoid excessive density increase, the composites possess thermal conductivity up to 0.86±0.14 W/(m•K), which is 374% of that for neat polymer matrix. The synergistic thermal enhancement from 1D+2D hybrid materials becomes more distinct due to the uniform distribution of more expanded CNTs within hybrid network. Both techniques show better performance compared to control samples fabricated by direct-mixing. This study paves the way for thermally conductive polymer composites used as thermal interface materials for next-generation electronic packaging and 3D integration circuits, particularly when both directional thermal conduction and complex composite geometry are simultaneously required.

Acknowledgements

Funding: This work was partially supported by the National Key R&D Program of China (Grant Nos. 2018YFA0208402, 2020YFA0714700), the National Natural Science Foundation of China (Grant Nos. 52172060, 51820105002, 11634014 and 51372269), Magna International, and EPSRC project 'Advanced Nanotube Application and Manufacturing (ANAM) Initiative' [grant numbers EP/M015211/1]. General: The authors especially thank Mr. David Paul, Ms. Mingzhao Wang, Ms. Rulan Qiao, Dr. Sarah Stevenson, for their kind support and useful discussion.

Electronic Supplementary Material: Supplementary material (further details of 3D printed cage component, the in situ polymerization with vacuum bag method, thermal conductivity measurement setup and its mechanism, evolution of CNTSU and its composites with growth time, graphene-based hybrid fillers) is available in the online version of this article at http://dx.doi.org/10.1007/s12274-***-****-* (automatically inserted by the publisher).

References

Reference

[1] Pernot, G.;Stoffel, M.;Savic, I.;Pezzoli, F.;Chen, P.;Savelli, G.;Jacquot, A.;Schumann, J.;Denker, U.;Mönch, I.;Deneke, C.;Schmidt, O. G.;Rampnoux, J. M.;Wang, S.;Plissonnier, M.;Rastelli, A.;Dilhaire, S.; Mingo, N. Precise control of thermal conductivity at the nanoscale through individual phonon-scattering barriers. *Nature Materials* **2010**, *9*, 491-495.

[2] Li, R.;Yang, X.;Li, J.;Shen, Y.;Zhang, L.;Lu, R.;Wang, C.;Zheng, X.;Chen, H.; Zhang, T. Review on polymer composites with high thermal conductivity and low dielectric properties for electronic packaging. *Materials Today Physics* **2022**, *22*, 100594.

[3] Song, Y.;Perez, C.;Esteves, G.;Lundh, J. S.;Saltonstall, C. B.;Beechem, T. E.;Yang, J. I.;Ferri, K.;Brown, J. E.;Tang, Z.;Maria, J.-P.;Snyder, D. W.;Olsson, R. H., III;Griffin, B. A.;Trolier-McKinstry, S. E.;Foley, B. M.; Choi, S. Thermal Conductivity of Aluminum Scandium Nitride for 5G Mobile Applications and Beyond. *ACS Applied Materials & Interfaces* **2021**, *13*, 19031-19041.

[4] Moore, A. L.; Shi, L. Emerging challenges and materials for thermal management of electronics. *Materials Today* **2014**, *17*, 163-174.

[5] Yu, A.;Ramesh, P.;Sun, X.;Bekyarova, E.;Itkis, M. E.; Haddon, R. C. Enhanced Thermal Conductivity in a Hybrid Graphite Nanoplatelet – Carbon Nanotube Filler for Epoxy Composites. *Advanced Materials* **2008**, *20*, 4740-4744.

[6] Liang, Q.;Moon, K. S.;Jiang, H.; Wong, C. P. Thermal Conductivity Enhancement of Epoxy Composites by Interfacial Covalent Bonding for Underfill and Thermal Interfacial Materials in Cu/Low-K Application. *IEEE Transactions on Components, Packaging and Manufacturing Technology* **2012**, *2*, 1571-1579.

[7] Du, F.;Guthy, C.;Kashiwagi, T.;Fischer, J. E.; Winey, K.

I. An infiltration method for preparing single-wall nanotube/epoxy composites with improved thermal conductivity. *Journal of Polymer Science Part B: Polymer Physics* **2006**, *44*, 1513-1519.

[8] Marconnet, A. M.;Yamamoto, N.;Panzer, M. A.;Wardle, B. L.; Goodson, K. E. Thermal Conduction in Aligned Carbon Nanotube–Polymer Nanocomposites with High Packing Density. *ACS Nano* **2011**, *5*, 4818-4825.

[9] Bryning, M. B.;Milkie, D. E.;Islam, M. F.;Kikkawa, J. M.; Yodh, A. G. Thermal conductivity and interfacial resistance in single-wall carbon nanotube epoxy composites. *Applied Physics Letters* **2005**, *87*, 161909.

[10] Biercuk, M. J.;Llaguno, M. C.;Radosavljevic, M.;Hyun, J. K.;Johnson, A. T.; Fischer, J. E. Carbon nanotube composites for thermal management. *Applied Physics Letters* **2002**, *80*, 2767-2769.

[11] Gojny, F. H.;Wichmann, M. H. G.;Fiedler, B.;Kinloch, I. A.;Bauhofer, W.;Windle, A. H.; Schulte, K. Evaluation and identification of electrical and thermal conduction mechanisms in carbon nanotube/epoxy composites. *Polymer* **2006**, *47*, 2036-2045.

[12] Hu, J.;Huang, Y.;Yao, Y.;Pan, G.;Sun, J.;Zeng, X.;Sun, R.;Xu, J.-B.;Song, B.; Wong, C.-P. Polymer Composite with Improved Thermal Conductivity by Constructing a Hierarchically Ordered Three-Dimensional Interconnected Network of BN. *ACS Applied Materials & Interfaces* **2017**, *9*, 13544-13553.

[13] He, H.;Peng, W.;Liu, J.;Chan, X. Y.;Liu, S.;Lu, L.; Le Ferrand, H. Microstructured BN Composites with Internally Designed High Thermal Conductivity Paths for 3D Electronic Packaging. *Advanced Materials* **2022**, *34*, 2205120.

[14] Han, W.;Bai, Y.;Liu, S.;Ge, C.;Wang, L.;Ma, Z.;Yang, Y.; Zhang, X. Enhanced thermal conductivity of commercial polystyrene filled with core-shell structured BN@PS. *Composites Part A: Applied Science and Manufacturing* **2017**, *102*, 218-227.

[15] Lin, Z.;Liu, Y.;Raghavan, S.;Moon, K.-s.;Sitaraman, S. K.; Wong, C.-p. Magnetic Alignment of Hexagonal Boron Nitride Platelets in Polymer Matrix: Toward High Performance Anisotropic Polymer Composites for Electronic Encapsulation. *ACS Applied Materials & Interfaces* **2013**, *5*, 7633-7640.

[16] Wang, X.-B.;Weng, Q.;Wang, X.;Li, X.;Zhang, J.;Liu, F.;Jiang, X.-F.;Guo, H.;Xu, N.;Golberg, D.; Bando, Y. Biomass-Directed Synthesis of 20 g High-Quality Boron Nitride Nanosheets for Thermoconductive Polymeric Composites. *ACS Nano* **2014**, *8*, 9081-9088.

[17] Kinloch, I. A.;Suhr, J.;Lou, J.;Young, R. J.; Ajayan, P. M. Composites with carbon nanotubes and graphene: An outlook. *Science* **2018**, *362*, 547-553.

[18] Shenogina, N.;Shenogin, S.;Xue, L.; Keblinski, P. On the lack of thermal percolation in carbon nanotube composites. *Applied Physics Letters* **2005**, *87*.

[19] Zhang, X.;Tan, W.;Smail, F.;De Volder, M.;Fleck, N.; Boies, A. High-fidelity characterization on anisotropic thermal conductivity of carbon nanotube sheets and on their effects of thermal enhancement of nanocomposites. *Nanotechnology* **2018**, *29*, 365708.

[20] Zhong, S.-L.;Zhou, Z.-Y.;Zhang, K.;Shi, Y.-D.;Chen, Y.-F.;Chen, X.-D.;Zeng, J.-B.; Wang, M. Formation of thermally conductive networks in isotactic polypropylene/hexagonal boron nitride composites via "Bridge Effect" of multi-wall carbon nanotubes and graphene nanoplatelets. *RSC Advances* **2016**, *6*, 98571-98580.

[21] Im, H.; Kim, J. Thermal conductivity of a graphene oxide–carbon nanotube hybrid/epoxy composite. *Carbon* **2012**, *50*, 5429-5440.

[22] de La Verpilliere, J.;Jessl, S.;Saeed, K.;Ducati, C.;De Volder, M.; Boies, A. Continuous flow chemical vapour deposition of carbon nanotube sea urchins. *Nanoscale* **2018**, *10*, 7780-7791.

[23] Carey, T.;Cacovich, S.;Divitini, G.;Ren, J.;Mansouri, A.;Kim, J. M.;Wang, C.;Ducati, C.;Sordan, R.; Torrisi, F. Fully inkjet-printed two-dimensional material field-effect heterojunctions for wearable and textile electronics. *Nature Communications* **2017**, *8*, 1202.

[24] Zhang, Y.-G.;Zhu, Y.-J.;Chen, F.; Sun, T.-W. Biocompatible, Ultralight, Strong Hydroxyapatite Networks Based on Hydroxyapatite Microtubes with Excellent Permeability and Ultralow Thermal Conductivity. *ACS Applied Materials & Interfaces* **2017**, *9*, 7918-7928.

[25] Bozlar, M.;He, D.;Bai, J.;Chalopin, Y.;Mingo, N.; Volz, S. Carbon Nanotube Microarchitectures for Enhanced Thermal Conduction at Ultralow Mass Fraction in Polymer Composites. *Advanced Materials* **2010**, *22*, 1654-1658.

[26] Nan, C.-W.;Birringer, R.;Clarke, D. R.; Gleiter, H. Effective thermal conductivity of particulate

composites with interfacial thermal resistance. *Journal of Applied Physics* **1997**, *81*, 6692-6699.

[27] Datta, S. S.;Strachan, D. R.;Khamis, S. M.; Johnson, A. T. C. Crystallographic Etching of Few-Layer Graphene. *Nano Letters* **2008**, *8*, 1912-1915.

[28] Lukas, M.;Meded, V.;Vijayaraghavan, A.;Song, L.;Ajayan, P. M.;Fink, K.;Wenzel, W.; Krupke, R. Catalytic subsurface etching of nanoscale channels in graphite. *Nature Communications* **2013**, *4*, 1379.

[29] Jo, I.;Pettes, M. T.;Kim, J.;Watanabe, K.;Taniguchi, T.;Yao, Z.; Shi, L. Thermal Conductivity and Phonon Transport in Suspended Few-Layer Hexagonal Boron Nitride. *Nano Letters* **2013**, *13*, 550-554.

[30] Pak, S. Y.;Kim, H. M.;Kim, S. Y.; Youn, J. R. Synergistic improvement of thermal conductivity of thermoplastic composites with mixed boron nitride and multi-walled carbon nanotube fillers. *Carbon* **2012**, *50*, 4830-4838.

[31] Sato, K.;Horibe, H.;Shirai, T.;Hotta, Y.;Nakano, H.;Nagai, H.;Mitsuishi, K.; Watari, K. Thermally conductive composite films of hexagonal boron nitride and polyimide with affinity-enhanced interfaces. *Journal of Materials Chemistry* **2010**, *20*, 2749-2752.

[32] Kelly, A. G.;O'Suilleabhain, D.;Gabbett, C.; Coleman, J. N. The electrical conductivity of solution-processed nanosheet networks. *Nature Reviews Materials* **2022**, *7*, 217-234.

[33] Bonnet, P.;Sireude, D.;Garnier, B.; Chauvet, O. Thermal properties and percolation in carbon nanotube-polymer composites. *Applied Physics Letters* **2007**, *91*.

[34] Liu, Y.;Ong, Z.-Y.;Wu, J.;Zhao, Y.;Watanabe, K.;Taniguchi, T.;Chi, D.;Zhang, G.;Thong, J. T. L.;Qiu, C.-W.; Hippalgaonkar, K. Thermal Conductance of the 2D MoS2/h-BN and graphene/h-BN Interfaces. *Scientific Reports* **2017**, *7*, 43886.

[35] Guthy, C.;Du, F.;Brand, S.;Winey, K. I.; Fischer, J. E. Thermal Conductivity of Single-Walled Carbon Nanotube/PMMA Nanocomposites. *Journal of Heat Transfer* **2007**, *129*, 1096-1099.

Electronic Supplementary Material

Enhanced composite thermal conductivity by presetting interconnected networks of in situ confined-grown carbon nanotubes

Xiao Zhang[1,2] (✉), Wei Tan[2,†], Tian Carey[3,§], Bo Wen[2,3,‡], Delong He[4], Adrees Arbab[3], Alex Groombridge[2,5], Fiona Smail[2], Jean de La Verpilliere[2,5], Chengning Yao[6], Yanchun Wang[1], Xiaojun Wei[1], Huaping Liu[1], Sishen Xie[1], Felice Torrisi[3,6,7], Michael De Volder[2] (✉), Weiya Zhou[1](✉), Adam Boies[2] (✉)

[1] *Beijing National Laboratory for Condensed Matter Physics, Institute of Physics, Chinese Academy of Sciences, Beijing, 100190, China.*
[2] *Department of Engineering, University of Cambridge, Cambridge, CB2 1PZ, UK.*
[3] *Cambridge Graphene Centre, Engineering Department, University of Cambridge, Cambridge, CB3 0FA, UK.*
[4] *Université Paris-Saclay, Centrale-Supélec, ENS Paris-Saclay, CNRS, LMPS - Laboratoire de Mécanique Paris-Saclay, 91190, Gif-sur-Yvette, France.*
[5] *Echion Technologies, Cambridge, CB22 3FG, UK.*
[6] *Molecular Sciences Research Hub, Imperial College London, London, W12 0BZ, UK.*
[7] *Dipartimento di Fisica e Astronomia, Universita' di Catania, Catania, 64 95123, Italy.*
† *Present address: School of Engineering and Materials Science, Queen Mary University of London, London, E1 4NS, UK.*
‡ *Present address: Jaguar Land Rover, Banbury Road Gaydon, Lighthorne Heath, Warwick, CV35 0RR, UK.*
§ *Present address: School of Physics, CRANN & AMBER Research Centres, Trinity College Dublin, Dublin, D02 E8C0, Ireland.*

Supporting information to DOI 10.1007/s12274-****-****-* (automatically inserted by the publisher)

Address correspondence to X. Zhang, zhangx@iphy.ac.cn; M. De Volder, mfld2@cam.ac.uk; W. Zhou, wyzhou@iphy.ac.cn; A. Boies, amb233@cam.ac.uk

Figure S1 The 3D printed cage component precursors. After trimming and polishing, the cage components were baked to remove the wax composition in the resin and partially anneal the SiO2 to get an integrated part (1100℃ resistance).

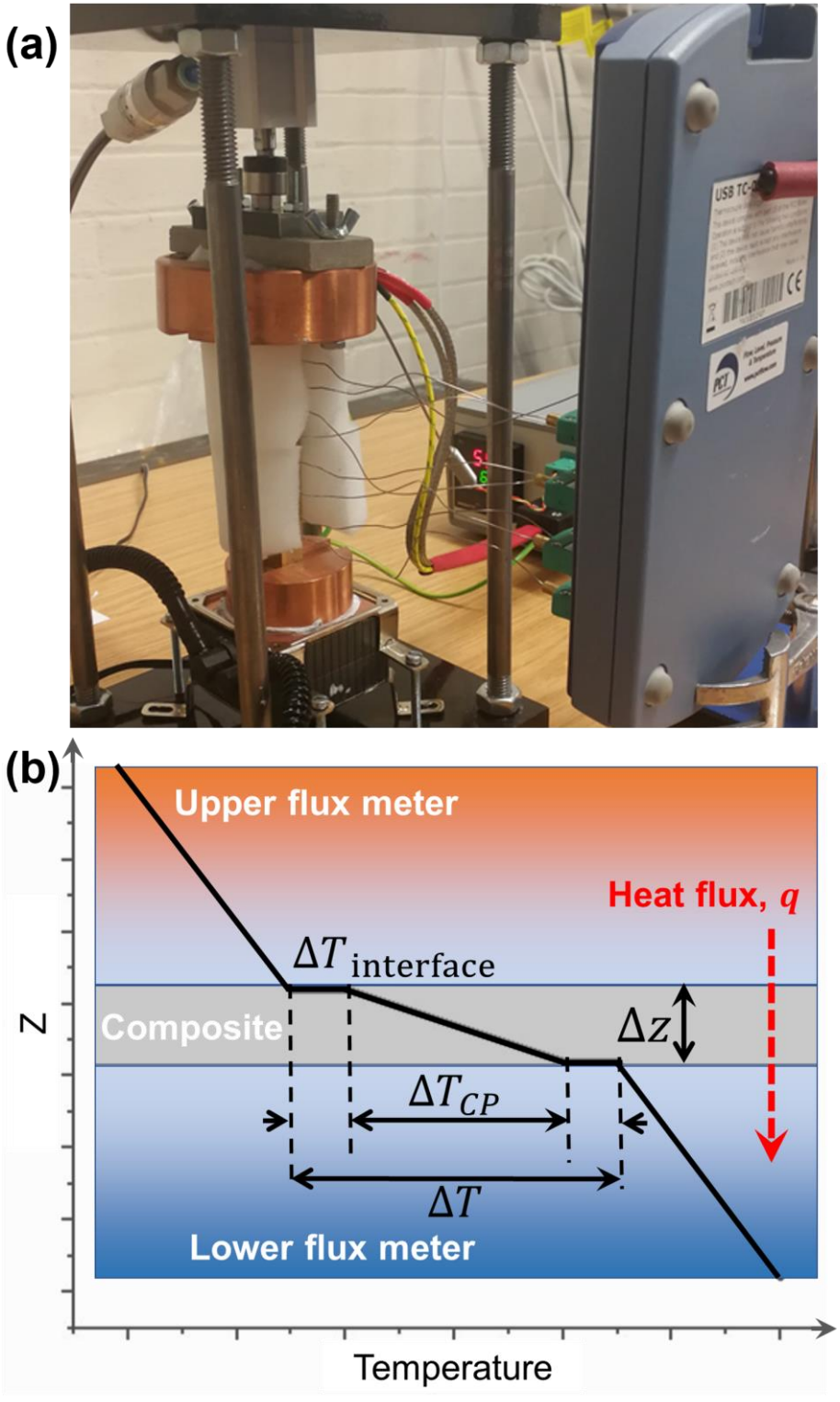

Figure S2 Thermal conductivity measurement setup and its mechanism. (a) Photo of the device during measurement. Two pieces of copper blocks were used as heat flux meters at hot and cold end, from which the temperature profiles were recorded by eight inserted thermal couples. (b) Schematic depicting the temperature profiles of Bi-substrates technique [19]. Among specimens from the same batch but with different thicknesses, the consistency and minimizing of R_i was guaranteed by the same pneumatic pressure exerted on the specimen (0.6 MPa), same specimen polishing process, and the usage of same silicone thermal interface putty. The setup is thermally isolated with polymer foam to have one-dimensional heat flow along the copper blocks and the specimen. Before the formal measurement, the setup had been calibrated by measuring stainless steel 304 foil (Alfa Aesar 41583, 42255, 41585). Under the standard procedure, the thermal conductivity of the 304 stainless steel is measured as 16.3±1.8 W/(m•K), very close to the value provided by the manufacturer 16.2 W/(m•K).

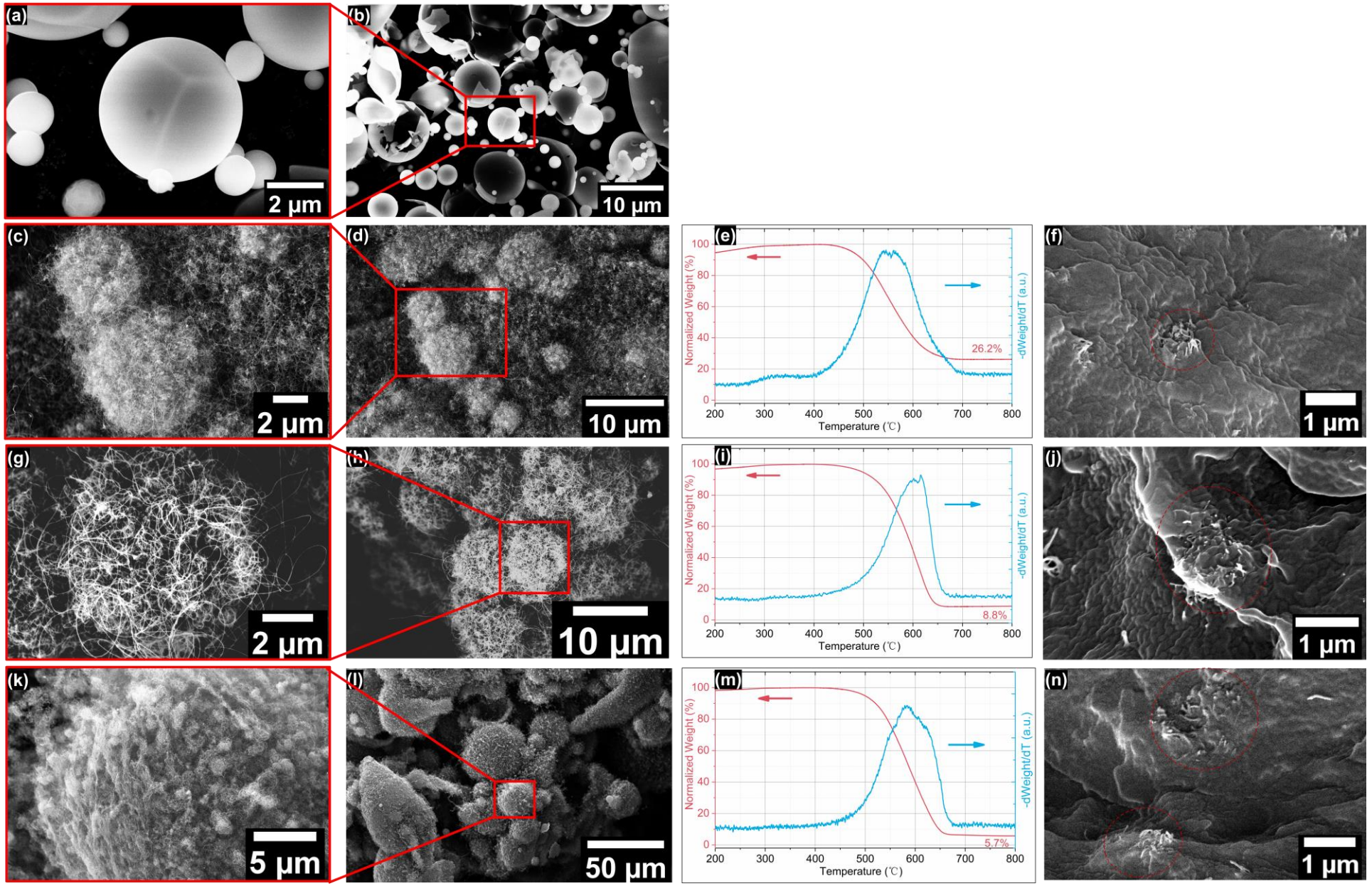

Figure S3 By increasing growth time, CNTSU morphology and their final state in composites evolve. (a-b) The alloy micron cores of aluminium and iron oxides synthesized with a continuous aerosol process. With (c-d) 0.3 h, (g-h)1 h ,and (k-l) 4 h of CNT growth without any space confinements (free growth), the size of CNTSU expanded from 2-4 μm to >10 μm, nearly 10 times larger than the cores used. Meanwhile, based on the thermogravimetric analysis (TGA) results, the CNT percentage within CNTSU changes from ~73.8 %, ~91.2 %, ~94.3% and ~40% for (e) 0.3 h, (i) 1 h, (m) 4 h of growth and in-line continuous growth [22], respectively (fraction of maximum weight (red, left axis) and relative weight variation rate (blue, right axis)). The weight of oxidized cores nearly did not change from 100-700 ℃[22]. Considering the major weight loss of CNTSU occured in the range of 450 – 600 ℃ in air, the CNTs whithin CNTSU seem pure with little amorphous carbon. (f, j, n) By direct-mixing 2 wt% CNTSU within matrix, CNTSUs were isolated distributed regardless of growth time.

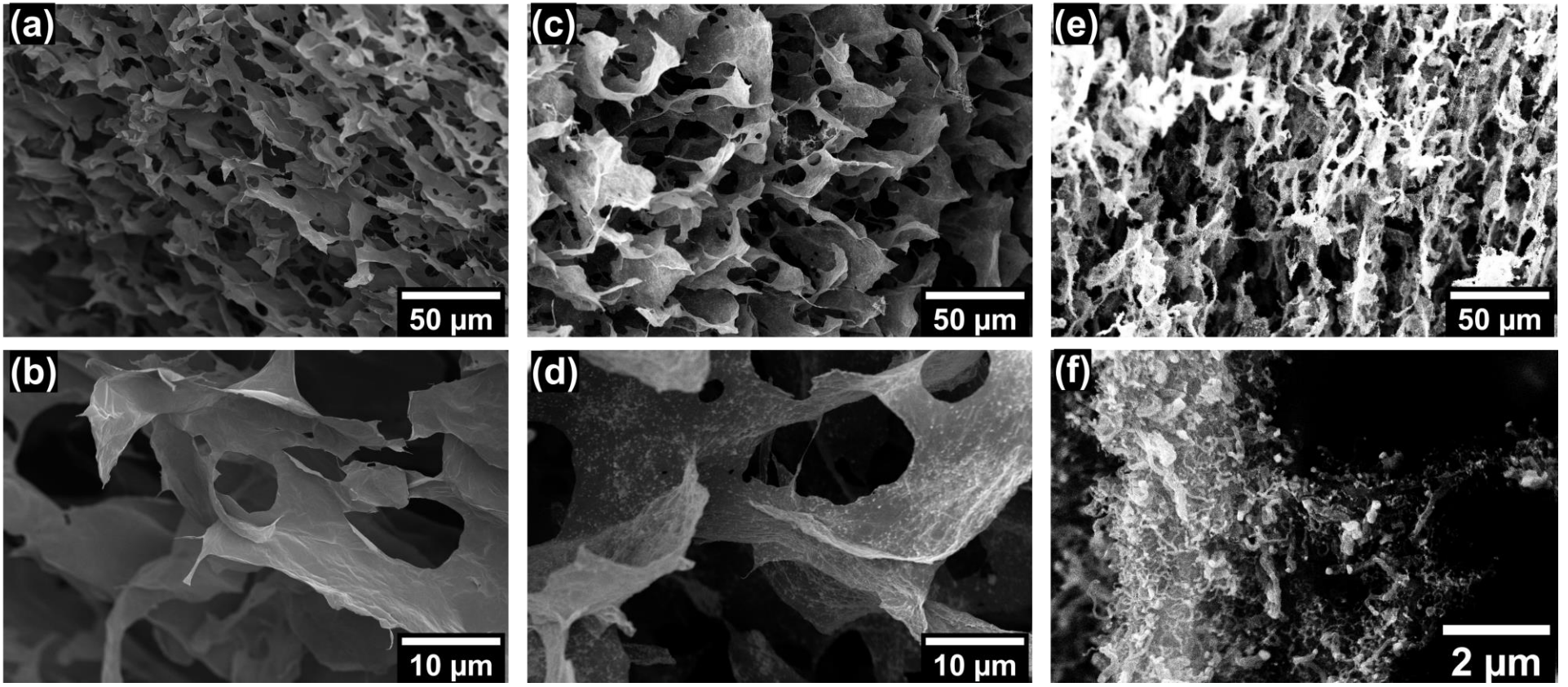

Figure S4 In situ grown CNT-rGO aligned network used as thermal hybrid fillers. (a-b) Based on GO solution and directional ice-templating self-assembly method, the aligned GO networks were prepared. The GO network was further reduced in hydrogen at 800 ℃ to obtain rGO network. (c-d) By adding Fe_2O_3 NP within GO solution and following the same procedure, the iron catalysts@rGO network was prepared. With further in situ CVD growth, CNTs synthesized from iron catalysts within rGO network. However, to build a CNT-graphene carbon 1D+2D thermal conduction network, we have not achieved any competitive results (brown solid pentagon in Figure 8). After in situ CNT growth, the thermal enhancement from the hybrid filler seemed even worse if did exist when compared with that from rGO aligned network (brown hollow pentagon). Iron catalysts seem to deteriorate the graphene surface by etching at high temperature and reduction environment.